LAWRENCE
LIVERMORE
NATIONAL
LABORATORY

UCRL-JRNL-210299

Crystal stability and equation of state for americium: theory

P. Soderlind, A. Landa

March 8, 2005

Physical Review B

Crystal stability and equation of state for americium: theory

P. Söderlind and A. Landa

Lawrence Livermore National Laboratory,

University of California, P.O. Box 808, Livermore, CA 94550

(Dated: March 8, 2005)

Abstract

Density-functional electronic-structure calculations for americium metal concur with the recent reinterpretation of its high pressure phases (AmIII and AmIV). The pressure-induced increased dominance of $5f$-electron bonding (delocalization) is well described by electronic-structure calculations when electron spin and orbital correlations are considered. Also the calculated equation of state (EOS) agrees with experimental findings to a degree typically found for simpler metals. Am is known to adopt low symmetry crystal structures at 10 GPa (AmIII: face-centered orthorhombic) and 16 GPa (AmIV: primitive orthorhombic). These transitions are reproduced by theory with a remarkable accuracy (11 and 16 GPa). At higher compression (60%) theory predicts a new bcc phase, AmV, to be stable. We argue that the AmI phase is stabilized by contributions from the d shell to the cohesion whereas all other phases follow from $5f$-electron bonding. AmIV has often been associated with the face-centered orthorhombic α-U phase, which was its original interpretation. We show that AmIV is in fact closely related to the α-Np structure which is of the same type (primitive orthorhombic). This distinction is important and explain the believed discord between theory and experiment for AmIV in the past.

PACS numbers: 64.30.+t,64.70.Kb,71.20

I. INTRODUCTION

The physics of the actinide metals is challenging both experimentally and theoretically. Many of their physical properties depend largely on the $5f$ electrons contribution to the chemical bonding. The $5f$-electron states form narrow bands close to the Fermi level which provide an inherently unstable situation. Consequently, external parameters such as pressure and temperature, as well as chemical alloying, can have a substantial influence on the properties of the actinides. The early actinides, Th-Pu, have a parabolic volume decrease with atomic number while at the same time condensing in increasingly complex structures. The atomic density reflects the integrated attractive bond contribution from the $5f$ electrons, whereas the condensed crystal is much more sensitive to details of the electronic structure. The structures have low symmetry because the $5f$ bands are pushed to unfavorable high and often degenerate energy levels when confined to high symmetry configurations.[1] In the heavier actinides, Am and on, the $5f$ bands are sufficiently narrow that their small mutual overlap poses a negligible influence on both atomic density and crystal structure. Applied pressure will eventually increase this overlap and changes in the atomic density and crystal structure are expected to occur. This scenario has its analog in the rare-earth metal series and one example is Pr for which experimental[2,3] and theoretical[4] studies have been presented.

For americium, several experimental studies have focused on the structural behavior under pressure.[5–10] They all agree that AmI and AmII are double hexagonal close-packed (dhcp) and face-centered cubic (fcc), respectively, but the transition pressures as well as the structural assignments of AmIII and AmIV have been controversial and confusing.[11] For instance, AmIII was suggested to be monoclinic and AmIV the face-centered orthorhombic (α-U) phase. Both these assignments were, however, later ruled out by first-principles theoretical predictions.[11] Instead possible candidates for the AmIV phase were suggested to be either the α-Np structure (primitive orthorhombic (po) with the space group Pnma) or the more complex α-Pu structure. Clearly, new experiments were needed to resolve the situation, and the latest findings suggest an AmI $\rightarrow$ AmII phase transition at 61 kbar, AmIII to be a plutonium structure (γ-Pu), i.e., a face-centered orthorhombic structure (fco) with a space group Fddd, and AmIV to be a po.[12] Although these measurements confirmed the possibility of the Pnma structure (thus ruling out the α-U structure) for AmIV, suggested by

theory,[11] the new AmIII phase was not foreseen in any earlier calculations. The experimental study[12] was limited to a highest pressure of 100 GPa (1 Mbar), but closer packed phases are expected beyond this pressure. The present calculations address this possibility.

Sect. II deals with details of our calculations and Sect. III present the results. Finally in Sect. IV and Sect. V we discuss our results and conclude.

II. COMPUTATIONAL DETAILS

The electronic structure and total energy are obtained from an all electron full-potential linear muffin-tin orbitals method (FPLMTO). This implementation has been used extensively and successfully for transition[13] and actinide[14] metals and allow for spin-orbit coupling, spin, and orbital polarization in the customary ways.[15–17] The "full potential" refers to the use of non-spherical contributions to the electron charge density and potential. This is accomplished by expanding these in cubic harmonics inside non-overlapping muffin-tin spheres and in a Fourier series in the interstitial region. We use two energy tails associated with each basis orbital and for Am's semi-core $6s$, $6p$, and valence $7s$, $7p$, $6d$, and $5f$ states, these pairs are different. Spherical harmonic expansions are carried out through $l_{max} = 6$ for the bases, potential, and charge density. For the electron exchange and correlation energy functional, the generalized gradient approximation (GGA) is adopted.[18]

As complementary tools we have used the so-called exact muffin-tin orbitals (EMTO) method as well as canonical band theory. The latter is simply an aid in guiding and analyzing the more complex self-consistent all electron calculations. The canonical bands are obtained from the canonical structure constants which are in turn derived from the LMTO method in the atomic sphere approximation.[19] The pure canonical band energies depend only on the crystal structure, l orbital quantum number, and the l-band occupation. These energies are element independent and can be used to study crystal-structure stabilities and their dependence on l-band occupation.

The calculations we have referred to as EMTO are performed using a fully relativistic Green's function technique based on the improved screened Korringa-Kohn-Rostoker (KKR) method, where the one-electron potential is represented by optimized overlapping muffin-tin (OOMT) potential spheres.[20–24] Inside the potential spheres the potential is spherically symmetric and it is constant between them. The radii of the potential spheres, the spher-

ical potentials inside them, and the constant value from the interstitial are determined by minimizing (i) the deviation between the exact and overlapping potentials and (ii) the errors coming from the overlap between spheres. Thus, the OOMT potential ensures a more accurate description of the full potential compared to the conventional muffin-tin or non-overlapping approach.

Within the EMTO formalism, the one-electron states are calculated *exactly* for the OOMT potentials. As an output of the EMTO calculations, one can determine the self-consistent Green's function of the system and the complete, non-spherically symmetric charge density. Finally, the total energy is calculated using the full charge density technique.[23,25] As in the case of the FPLMTO method, GGA is used for the exchange/correlation approximation. Spin-orbit coupling is taken into account exactly by solving the 4-component Dirac equation.[26] The EMTO calculations are performed for a basis set including valence *spdf* orbitals and the semi-core $6p$ state whereas the core states were recalculated at each iteration.

Integration over the irreducible wedge of the Brillouin zone (IBZ) is performed using the special k-point method[27] for both FPLMTO and EMTO. We used about 200 or more k points in the IBZ for all structures, except for the more complex (16 atoms/cell) α-Pu structure (16 k points).

All phases are assumed to be best described within an anti-ferromagnetic (AF) spin configuration with a total spin and orbital moment equal to zero. Test calculations for other spin configurations confirm this to give the lowest total energy, similar to the situation in Pu.[28] For dhcp (AmI) the spins are anti-parallel in the ABAC layers with the direction along the z-axis. The fcc phase (AmII) is set up as a super-cell with six atoms in a hexagonal cell, layered as ABCABC and anti-parallel spins in each layer. AmIII can be described with two atoms in a primitive cell of the fco unit cell. These two atoms have anti-parallel spins directed orthogonal to their respective plane. The po AmIV structure has 4 atoms/cell and again the spins are aligned anti-parallel. The monoclinic α-Pu structure, previously suggested theoretically as the AmIV phase[11,29] is assumed to have the spin configuration that is known to give the lowest total energy[30] for plutonium. For compressions where the bcc phase is found to be relevant, any spin polarization is completely suppressed.

The EOS for the respective phase is obtained from a fit of the total energies to a Murnaghan form.[31] Transition pressures are obtained numerically by fitting the total energies,

close to the transition, to a 4th degree polynomial and analytically differentiate this to obtain the pressure and the free energy. The transition is defined to occur when the Gibbs free energy

$$G = E + PV - TS = H - TS$$

for the phases intersect. The present calculations are subject to the Born-Oppenheimer approximation and are strictly valid at zero temperature (T=0).

III. RESULTS

Let us first address the ground-state phase of Am. Total energy calculations for the dhcp and fcc crystal structures reveal that theory is unable to distinguish between these two phases at ambient pressure. Fig. 1 shows that the total energy difference between dhcp and fcc is within error margin of the numerical calculation (often assumed to be about 1 mRy/atom). Hence, no reliable transition pressure between these two phases can be determined from the present calculations. It becomes clear, however, that compression is gradually stabilizing the fcc over the dhcp phase in accordance with the experimental phase diagram. The dhcp phase in Am has been argued to be stabilized by d-band contribution to the chemical bond,[11] similar to the rare-earth elements,[32] and we will discuss this further in Sect. IV.

Next, in Fig. 2, we focus on the stability of the AmII, AmIII, and AmIV phases and also compare with the monoclinic α-Pu phase. Clearly, the monoclinic phase is not stable compared to the recently established fco (AmIII) and po (AmIV) phases. It should be noted that the α-U structure is much higher in energy, thus very unstable, compared to any of the phases in Fig. 2. In this figure we also mark the calculated transitions AmII $\rightarrow$ AmIII at 107 kbar and AmIII $\rightarrow$ AmIV at 158 kbar, in agreement with the latest experimental data of 100 and 160 kbar, respectively.[12]

The AmIII phase is interestingly the same structure as the γ-Pu structure. It was recently shown[28] that density-functional theory could accurately account for all known Pu phases, with the total energy of the ϵ (bcc) phase being somewhat high. This could only be achieved when spin and orbital correlations were included in the model.[28] Therefore it is no surprise that this is the case also for AmIII. For AmIV, on the other hand, the spin moment is essentially quenched. The AmII $\rightarrow$ AmIII and AmIII $\rightarrow$ AmIV transitions are sensitive to relaxation effects of the AmIII structure. In Fig. 3 the relaxed axial ratios of AmIII is

plotted as function of the atomic volume, together with experimental data.[12] Notice that the quantitative behaviors of b/a and c/a compare well between theory and experiment. The b/a shows a relatively strong decrease with compression while the c/a is weakly increasing. By analyzing the electrostatic (Madelung) energies associated with these variations (not shown) it is clear that the lattice is increasingly distorted (farther from close-packed) with increasing compression. This is reasonable because the next phase (AmIV) is in this sense even more distorted.

The AmIV phase, now established by both experiment and theory, is not in discord with the previous calculations[11,29] because it is close to the α-Np structure which was determined as a particularly favorable phase in Am under the pressure. In Fig. 4 the AmIV unit cell (a) is almost identical to the α-Np unit cell (b), with a doubling of the AmIV cell along the z-axis. This way 4 and 8 atoms constitute the AmIV and the α-Np cell, respectively. If also the conventions of x and y axis are exchanged, and the repeat of the cell along the z axis is accounted for, the b/a and c/a axial ratios of the α-Np are close to those of the AmIV phase. The α-U structure has, however, significantly different axial ratios, compare Table I. These ratios remained nearly constant during the compression as calculated relaxation effects are very small in AmIV.

In Fig. 5 we show the computed EOS for AmII-AmIV together with the most recent available data[12] for AmI-AmIV. The theoretical EOS for AmI and AmII are practically indistinguishable at lower pressures, as mentioned, and therefore AmI is left out of the plot for clarity. V_0 is the ambient pressure atomic volume of the AmI phase and the same number (29.3 Å^3) is used for both theory and experiment. Notice that our parameter-free theory appears to agree with measured data, within experimental scatter, for AmII and AmIV. Also the unrelaxed calculation of AmIII compares very well with experimental data. The calculations for which the b/a and c/a axial ratios are relaxed show smaller volumes and an EOS that continuously matches onto the AmIV phase. This does not agree well with experiment and we believe that the distortion might be somewhat exaggerated in the calculations as perhaps also Fig. 3 suggests. For comparison we also performed EOS calculations in Fig. 6 for these phases by means of the EMTO method. These compares well with FPLMTO and measured data up to about 200 kbar. Beyond this pressure the EMTO calculations begin to deviate from experiment and we believe that the definition of the 6s state as a core state is breaking down at this point. Nevertheless, the EMTO is viable

at lower pressures and has the advantage of a very sophisticated treatment of the effect of alloying.[24]

The AmIV phase has been shown to be stable up to 1 Mbar (100 GPa) in the most recent experiments. Without a doubt, there must be a higher symmetry phase eventually stable in Am at sufficiently high compressions. Theoretical calculations[14] predicted some time ago that Th, Pa, U, Np, and Pu will crystallize in the hcp, hcp, bcc, bcc, and bcc structures, respectively. The reason is that the symmetry breaking mechanism that favors low symmetry structures will become less important as the $5f$ bands broaden[1] under compression. This, combined with the fact that electrostatic forces moves the atoms to higher symmetry positions, ensures a closer packed structure at high pressures. Canonical band theory, Sect. IV, suggests that bcc is a realistic high pressure phase in Am and we therefore completed calculations also for this phase. In Fig. 7 the energy difference between the AmIV and the bcc structures are plotted as a function of the atomic volume. At about 12 Å^3 (60% compression) bcc is stable over the AmIV phase. This is a transition from a very low symmetry to a very high symmetry structure which suggests that there might exist an intermediate phase, but none has yet been foreseen by theory.

IV. DISCUSSION

In the previous section we showed that the energies of the dhcp and the fcc phases were practically indistinguishable by theory. It is no argument experimentally, however, that dhcp is stable to about 60 kbar. This implies that dhcp Am should have a distinct but slightly lower energy than fcc Am at ambient pressure, which is not the case in the calculations. The present theory is unable to completely localize the $5f$ electrons and hence fully remove them from participating in the cohesion. The bonding is, however, substantially reduced by the fact that Am almost completely spin polarize in the calculations, see Fig. 8. Still this fact may explain why the dhcp and fcc Am have essentially degenerate total energies. To investigate this we have applied canonical band theory[19] to try and assess the individual d- and f-electron contribution to the fcc and dhcp stability in Am. The contributions from the diffuse s and p electrons are assumed to be negligible. In Fig. 9 we show the dhcp$-$fcc canonical energy difference for the d electrons. Notice that the d occupation of Am (~ 1.5) favor dhcp over fcc, in analogy to the trans-cerium rare-earth metals.[32] This corresponds to

a situation where the $5f$ electrons are fully removed from the bonding as is believed to be the case in Am, and the rare-earths, at ambient pressure.

Next, we plot the dhcp−fcc and bcc−fcc canonical energy differences for the f electrons in Fig. 10. We remember that the $5f$ band is spin polarized (Fig. 8) with about 6.6 spin up and 0.2 spin down electrons. The spin up/down f band can hold a maximum of 7 electrons, i.e., the spin up band is close to full and the spin down band nearly empty. For a spin degenerate band (holds 14 electrons) these occupations corresponds to 13.2 and 0.4, respectively. For these two occupations, marked in Fig. 10 with arrows, the canonical band theory suggests that fcc is stable with a small margin over dhcp. Hence, it seems plausible that the small amount of $5f$ contribution in our theoretical model of the ground-state of Am artificially favors fcc over dhcp such that, when the d contribution is included, their energies are degenerate. It is important to note that this implies that the fcc (AmII) phase is the first signal of $5f$-electron involvement in the Am phase diagram.

Lastly, in Fig. 10 we focus on the bcc−fcc canonical energy difference. The expected $5f$ occupation at high compression, where the spin is quenched, is about 6.7 and is marked in the figure. For this population of the canonical $5f$ band, the bcc phase is strongly favorable over the fcc phase and bcc therefore emerges as a possible high pressure phase in Am.

V. CONCLUSION

To summarize, we have investigated EOS and structural stability in Am metal up to Mbar pressure at ambient temperature. These calculations support the phase diagram recently reported.[12] In particular, theory for the AmII $\rightarrow$ AmIII and AmIII $\rightarrow$ AmIV transitions agree very well with measured data. Hence, the confusion in the literature regarding the AmIV phase seems to be resolved. Theory also predicts a new bcc phase to be stable at about 60% compression, yet to be confirmed by experiments. Analyzing the individual d- and f-electron contributions to the phase stability of Am suggests that all phases, except AmI, have $5f$ electron involvement.

Acknowledgments

B. Sadigh, J. Pask, L. Vitos, and A. Ruban are acknowledged for helpful discussions. This work was performed under the auspices of the U.S. Department of Energy by the University of California Lawrence Livermore National Laboratory under contract W-7405-Eng-48.

---

[1] P. Söderlind, O. Eriksson, B. Johansson, J.M. Wills, and A.M. Boring, Nature **374**, 524 (1995).

[2] B.J. Baer, H. Cynn, V. Iota, C.-S. Yoo, and G. Shen, Phys. Rev. B **67**, 134115 (2003).

[3] N.C. Cunningham, N. Velisavljevic, and Y.K. Vohra, Phys. Rev. B **71**, 012108 (2005).

[4] P. Söderlind, Phys. Rev. B **65**, 115105 (2002).

[5] J. Akella, Q. Johnson, W. Thayer, and R.N. Schock, J. Less-Common Met. **68**, 95 (1979).

[6] J. Akella, Q. Johnson, and R.N. Schock, J. Geophys. Res. B **85**, 7056 (1980).

[7] R.B. Roof, R.G. Haire, D. Stiffer, L.A. Schwalbe, E.A. Kmetko, and J.L. Smith, Science **207**, 1353 (1980).

[8] R.B. Roof, J. Appl. Crystallogr. **14**, 447 (1981).

[9] R.B. Roof, Z. Kristallogr. B **15**, 307 (1982).

[10] U. Benedict, J.P. Itie, C. Dufour, S. Dabs, and J.C. Sprite, in *Americium and Curium and Technology*, edited by N.M. Edelstein, J. Nervation, and W.W. Schmaltz (Redial, Dordrecht, 1985), pp. 221-224.

[11] P. Söderlind, R. Ahuja, O. Eriksson, B. Johansson, and J.M. Wills, Phys. Rev. B **61**, 8119 (2000).

[12] S. Heathman, R.G. Haire, T. Le Bihan, A. Lindbaum, K. Litfin, Y. Meresse, and H. Libotte, Phys. Rev. Lett. **85**, 2961 (2000); A. Lindbaum, S. Heathman, K. Litfin, Y. Meresse, R.G. Haire, T. Le Bihan, and H. Libotte, Phys. Rev. B **63**, 214101 (2001).

[13] R. Ahuja, P. Söderlind, J. Trygg, J. Melsen, J.M. Wills, B. Johansson, and O. Eriksson, Phys. Rev. B **50**, 14690 (1994).

[14] P. Söderlind, Adv. Phys. **47**, 959 (1998).

[15] O.K. Andersen, Phys. Rev. B **12**, 3060 (1975).

[16] O. Eriksson, M.S.S. Brooks, and B. Johansson, Phys. Rev. B **41**, 9087 (1990).

[17] P. Söderlind, Europhys. Lett. **55**, 525 (2001).

[18] J.P. Perdew, J.A. Chevary, S.H. Vosko, K.A. Jackson, M.R. Pederson, and D.J. Singh, Phys. Rev. B **46**, 6671 (1992); J.P. Perdew, K. Burke, and M. Ernzerhof, Phys. Rev. Lett. **87**, 156401 (2001).

[19] H.L. Skriver, Phys. Rev. B **31**, 1909 (1985).

[20] O.K. Andersen, O. Jepsen, and G. Krier, in *Methods of Electronic Structure Calculations,* edited by V. Kumar, O.K. Andersen, and A. Mookerjee (World Scientific, Singapore, 1994), pp. 6-124.

[21] O.K. Andersen, C. Arcangeli, R.W. Tank, T. Saha-Dasgupta, G. Krier, O. Jepsen, and I. Dasgupta, in *Tight-Binding Approach to Computational Materials Science*, edited by P.E.A. Turchi, A. Gonis, and L. Colombo, M. R. S. Symposia Proceedings No 491 (Materials Research Society, Warrendale, 1998), pp. 3-34.

[22] L. Vitos, H.L. Skriver, B. Johansson, and J. Kollar, Comput. Mater. Sci **18**, 24 (2000).

[23] L. Vitos, Phys. Rev. B **64**, 014107 (2001).

[24] L. Vitos, in *Recent Research and Development in Physics*, (Transworld Research Network Publisher, Trivandrum, 2004), Vol. 5, pp. 103-140.

[25] J. Kollar, L. Vitos, and H.L. Skriver, in *Electronic Structure and Physical Properties of Solids: The Uses of the LMTO Method*, edited by H. Dreysse, Lecture Notes in Physics Vol. 535 (Springer, Berlin, 2000), pp. 85-113.

[26] L. Pourovskii, A. Ruban, L. Vitos, E. Ebert, I. Abrikosov, and B. Johansson, Phys. Rev. B **71**, (2005) (to be published).

[27] D.J. Chadi and M.L. Cohen, Phys. Rev. B **8**, 5747 (1973); S. Froyen, *ibid.* **39**, 3168 (1989).

[28] P. Söderlind and B. Sadigh, Phys. Rev. Lett. **92**, 185702 (2004).

[29] M. Penicaud, J. Phys.: Condens. Matter **14**, 3575 (2002).

[30] B. Sadigh, P. Söderlind, and W.G. Wolfer, Phys. Rev. B **68**, 241101 (2003).

[31] F.D. Murnaghan, Proc. Natl. Acad. Sci. USA **30**, 244 (1944).

[32] J.C. Duthie and D.G. Pettifor, Phys. Rev. Lett. **38**, 564 (1977); A.K. McMahan, H.L. Skriver, and B. Johansson, Phys. Rev. B **23**, 5016 (1981).

Figures

FIG. 1: FPLMTO total energies (mRy/atom) for dhcp (AmI) and fcc (AmII) americium. Their energy difference at equilibrium, ΔE, is about 0.1 mRy/atom.

FIG. 2: FPLMTO total energy calculations (mRy/atom) for fcc (AmII), fco (AmIII), po (AmIV), and monoclinic (α-Pu) americium.

FIG. 3: Calculated and measured[12] b/a and c/a axial ratios of AmIII.

FIG. 4: The AmIV (a) and α-Np (b) structures. The AmIV cell is here repeated along the z direction to enable a direct comparison.

FIG. 5: FPLMTO and measured[12] EOS for Am. The symbols and lines represent the experimental data and theory, respectively. The dashed (fco) line corresponds to calculations where the axial ratios are allowed to relax. V_0 is the ambient pressure volume of Am, 29.3 Å^3.

FIG. 6: EMTO EOS for Am compared to experimental data.[12] The symbols and lines represent the experimental data and theory, respectively. V_0 is the ambient pressure volume of Am, 29.3 Å^3.

FIG. 7: AmIV – bcc calculated total energy difference in mRy/atom. Bcc becomes stable over AmIV at about 12 Å^3.

FIG. 8: Calculated DOS (states/eV/atom) for dhcp Am (AmI). The Fermi level is at zero Energy. Notice that the $5f$ spin-up band is nearly filled and the $5f$ spin-down band nearly empty. The s, p, and $6d$ DOS are all small, compared to the $5f$ DOS, in the vicinity of the Fermi level.

FIG. 9: Canonical d-band energy differences for dhcp relative to the fcc structure. The ambient pressure d-band population is marked by a vertical line.

FIG. 10: Canonical f-band energy differences for the dhcp and bcc structures, relative to the fcc structure. The vertical arrows show the location of the spin up (13.2) and down (0.4) $5f$ occupations in Am at ambient pressure and the $5f$, spin-degenerate, population (6.7) at high compression.

Tables

TABLE I: Axial ratios of AmIV, α-Np (primitive orthorhombic), and α-U (face-centered orthorhombic) at about 18 Å^3.

Phase	b/a	c/a
AmIV	0.92	0.60
α-Np	0.96	0.68
α-U	0.84	0.48

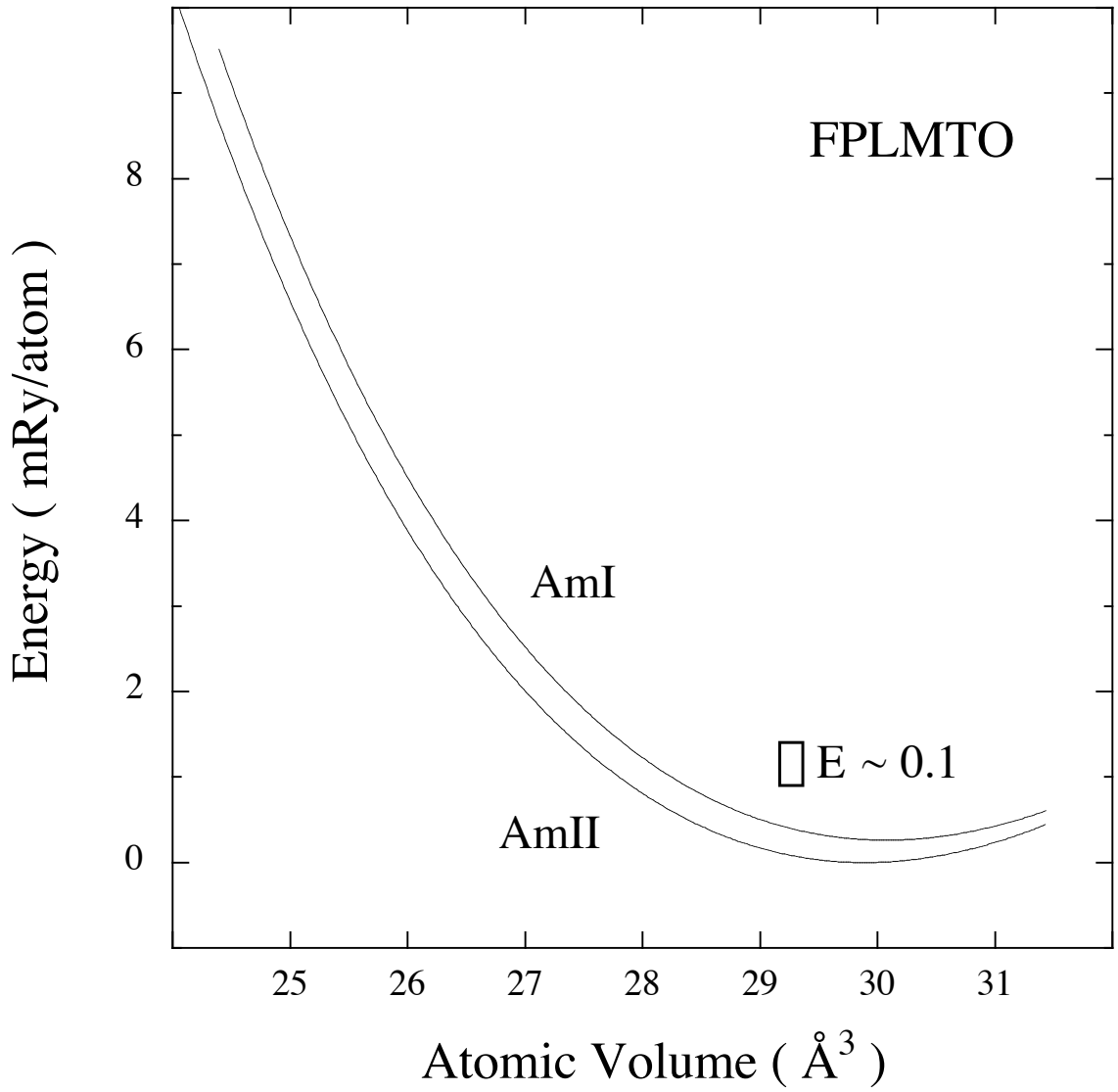
FPLMTO
AmI
AmII
E ~ 0.1
Energy (mRy/atom)
Atomic Volume (Å3)
0
2
4
6
8
25
26
27
28
29
30
31

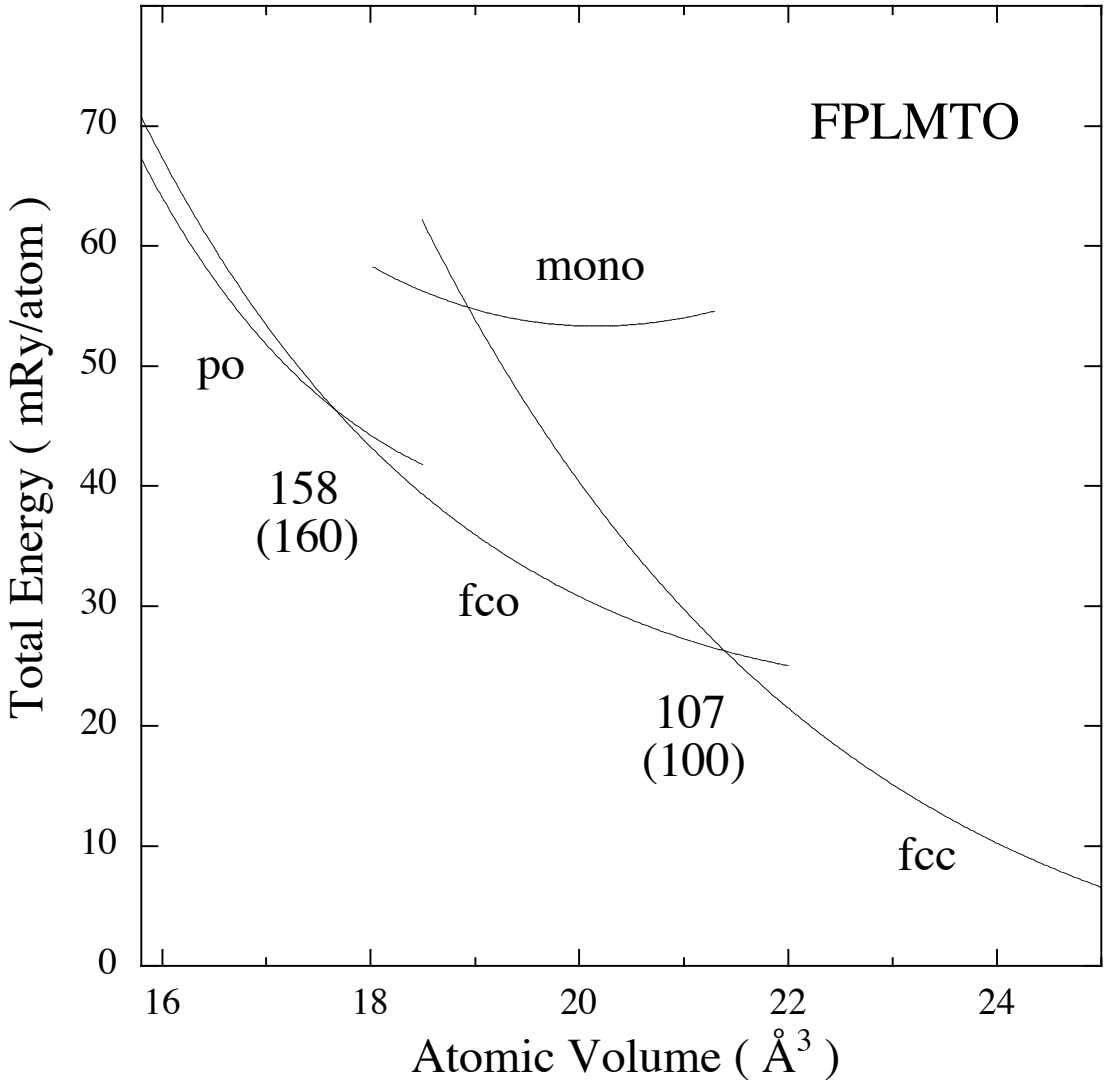
FPLMTO
mono
po
158
(160)
fco
107
(100)
fcc
Total Energy (mRy/atom)
Atomic Volume (Å^3)
0
10
20
30
40
50
60
70
16
18
20
22
24

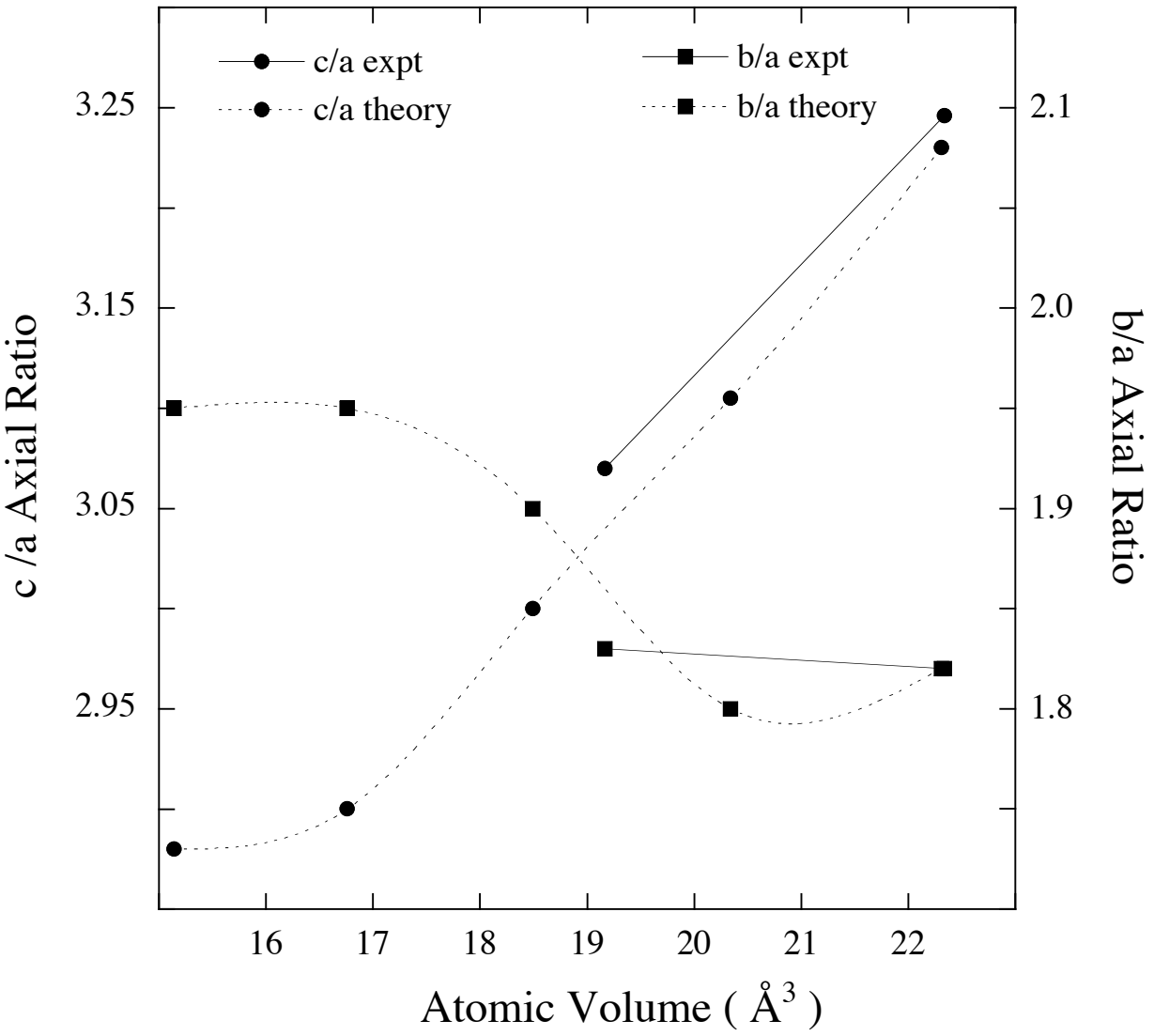
c/a expt
c/a theory
b/a expt
b/a theory
3.25
3.15
3.05
2.95
2.1
2.0
1.9
1.8
16
17
18
19
20
21
22
c /a Axial Ratio
b/a Axial Ratio
Atomic Volume (Å^3)

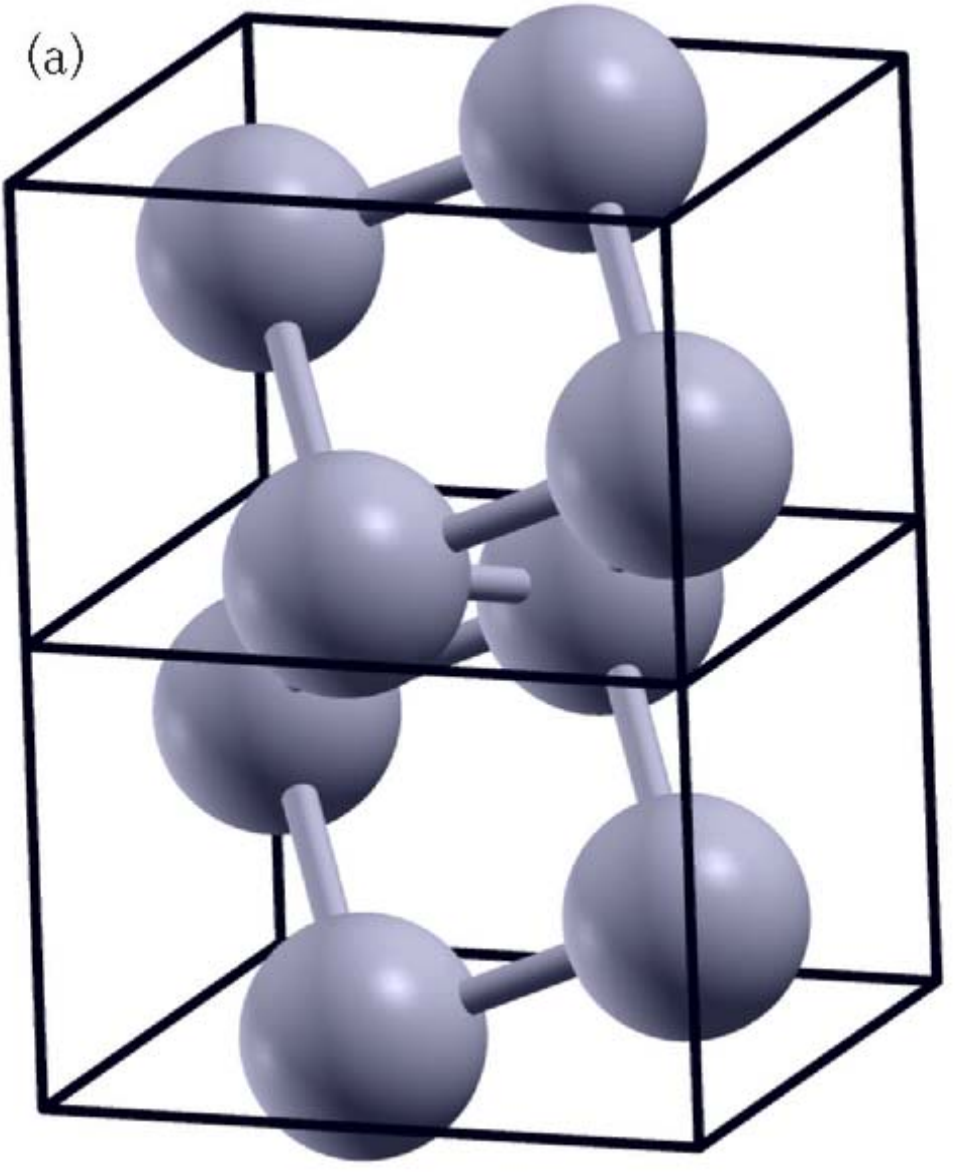
(a)

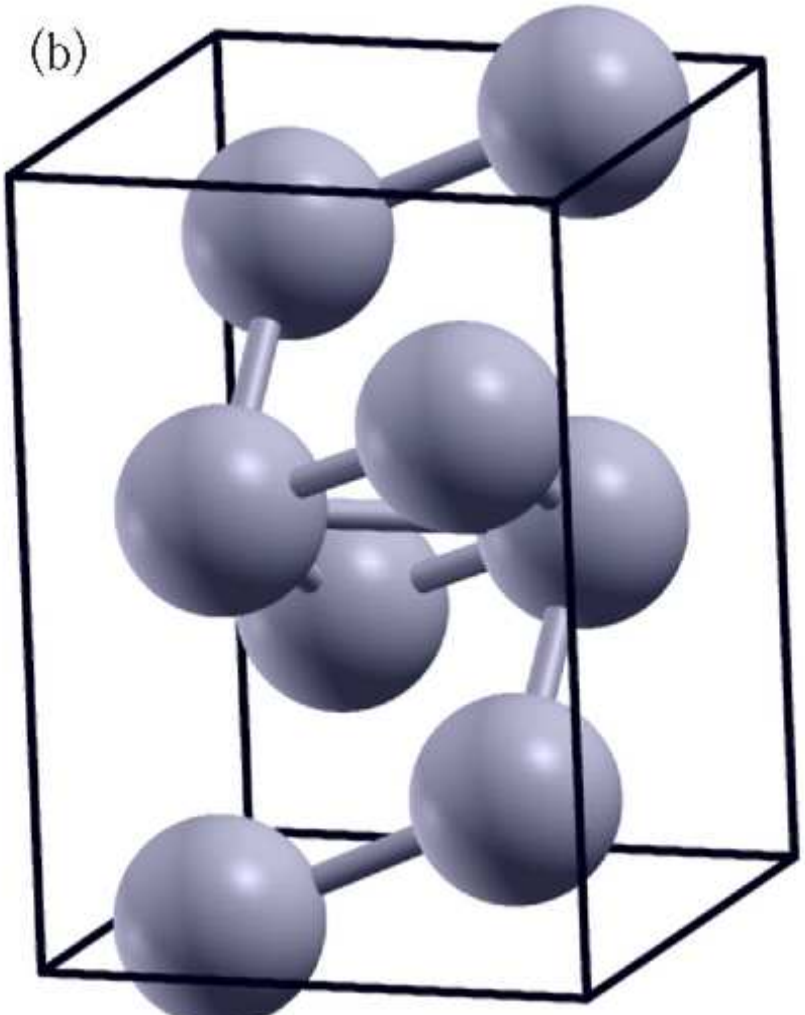
(b)

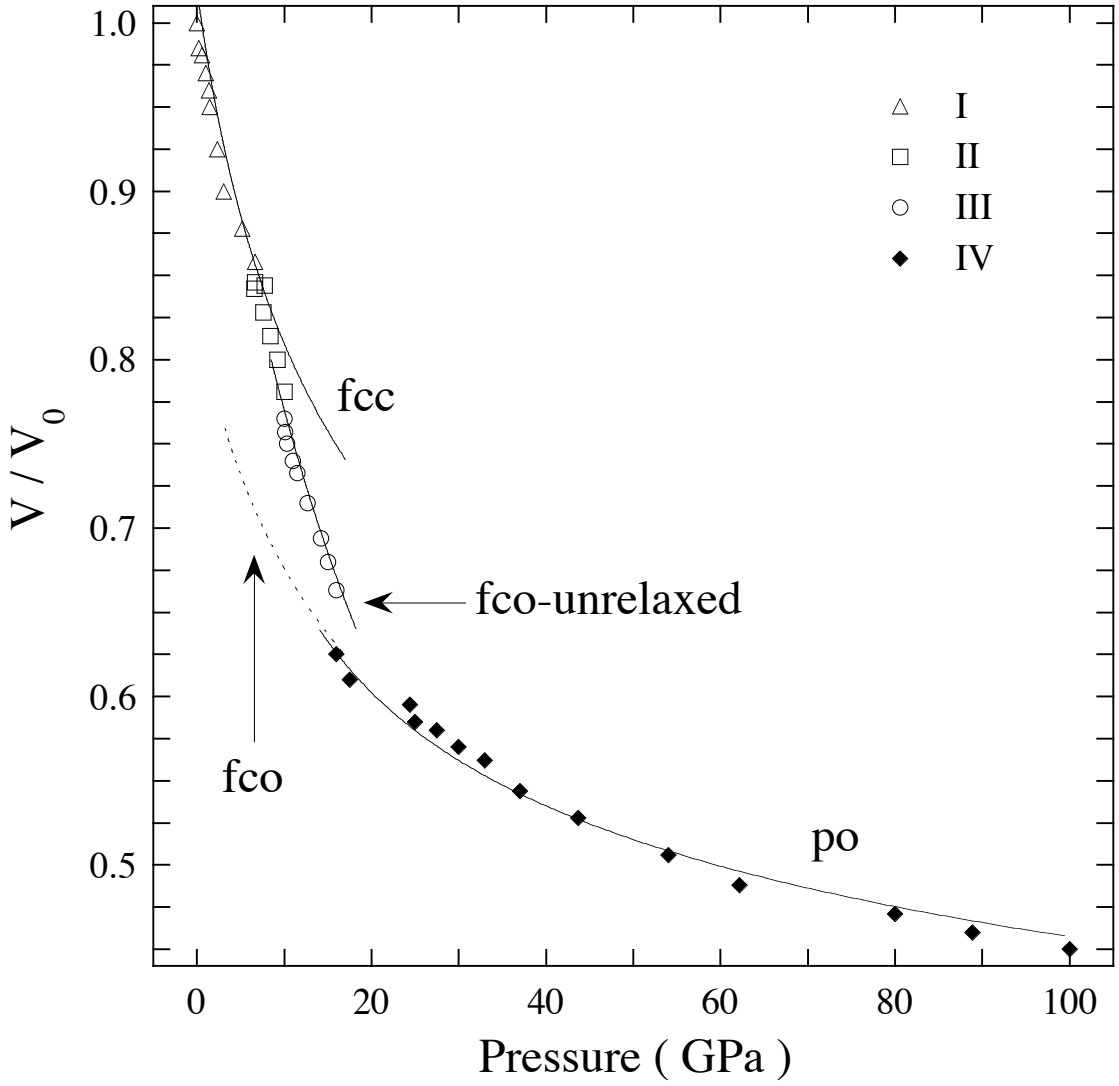
1.0
0.9
0.8
0.7
0.6
0.5
V / V0
0
20
40
60
80
100
Pressure (GPa)
I
II
III
IV
fcc
fco-unrelaxed
fco
po

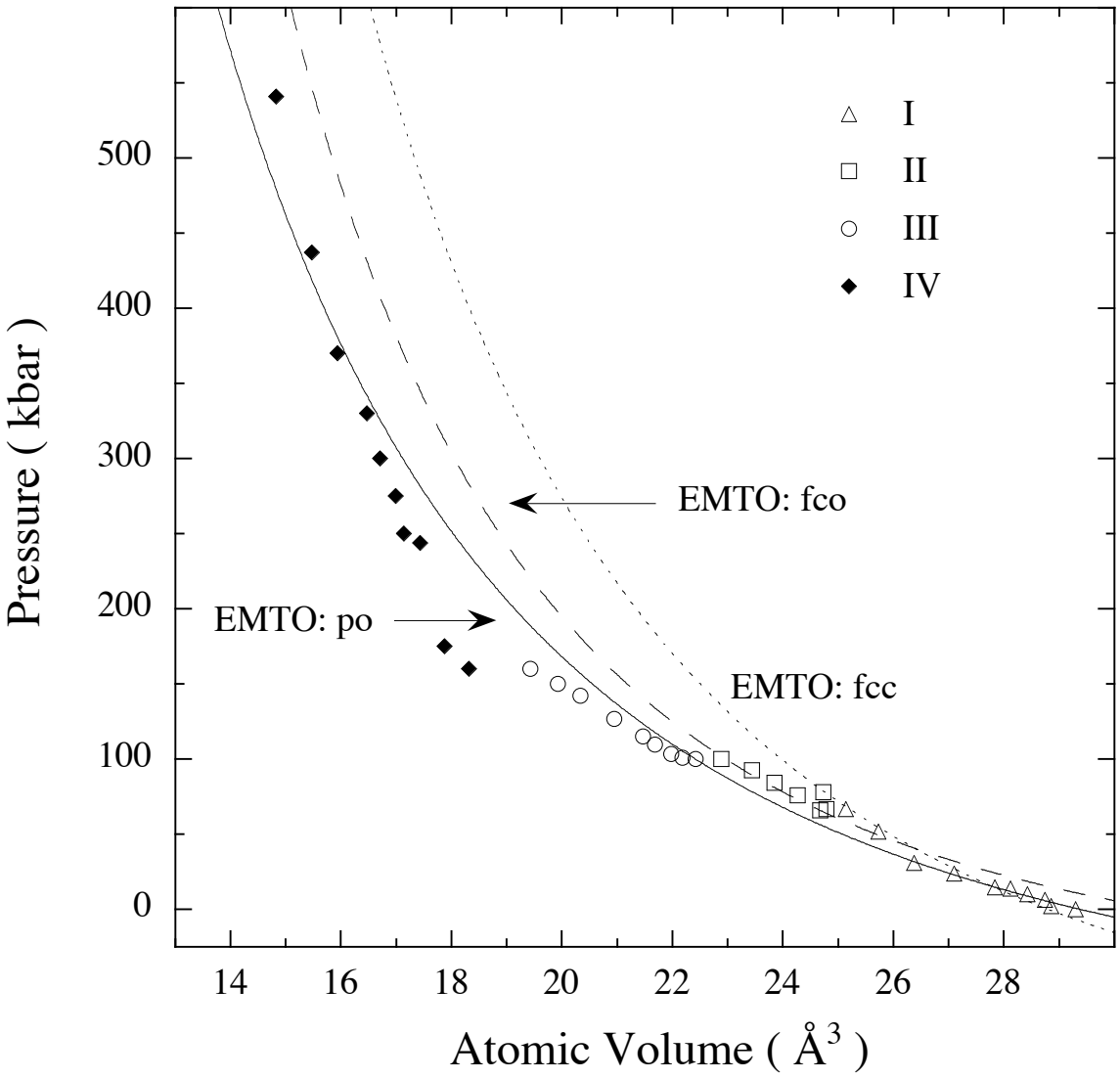
Pressure (kbar)
500
400
300
200
100
0
14
16
18
20
22
24
26
28
Atomic Volume (Å^3)
I
II
III
IV
EMTO: fco
EMTO: po
EMTO: fcc

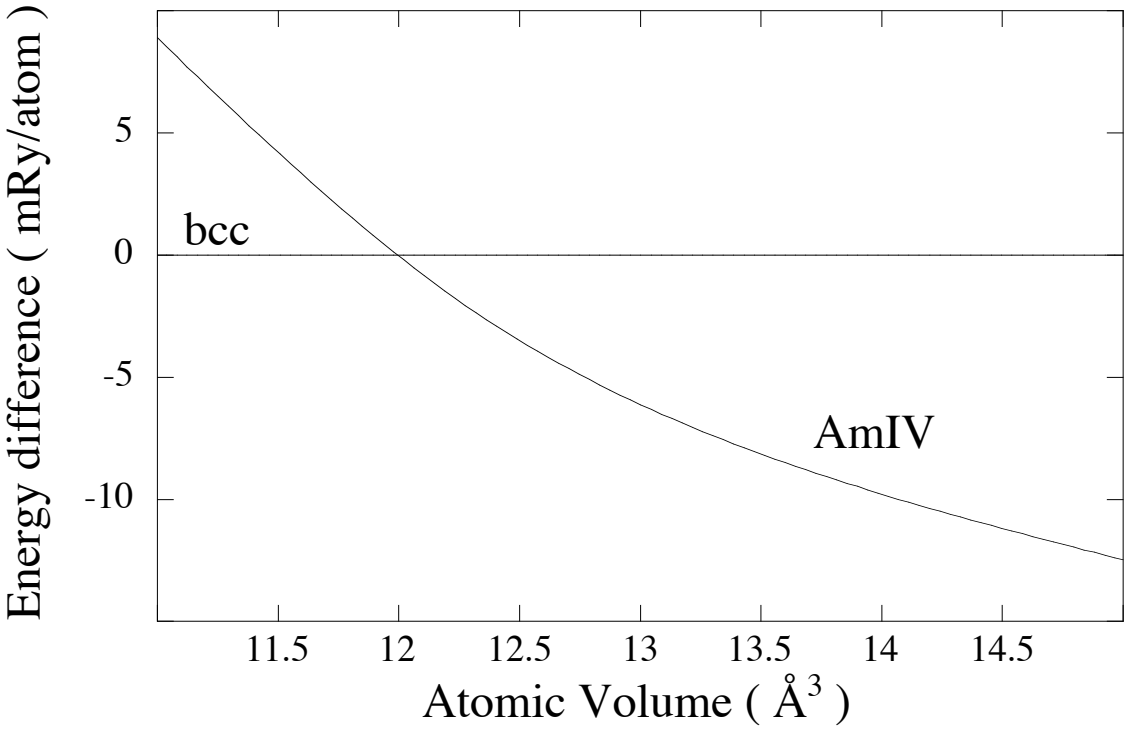
Energy difference (mRy/atom)
5
0
-5
-10
bcc
AmIV
11.5
12
12.5
13
13.5
14
14.5
Atomic Volume (Å^3)

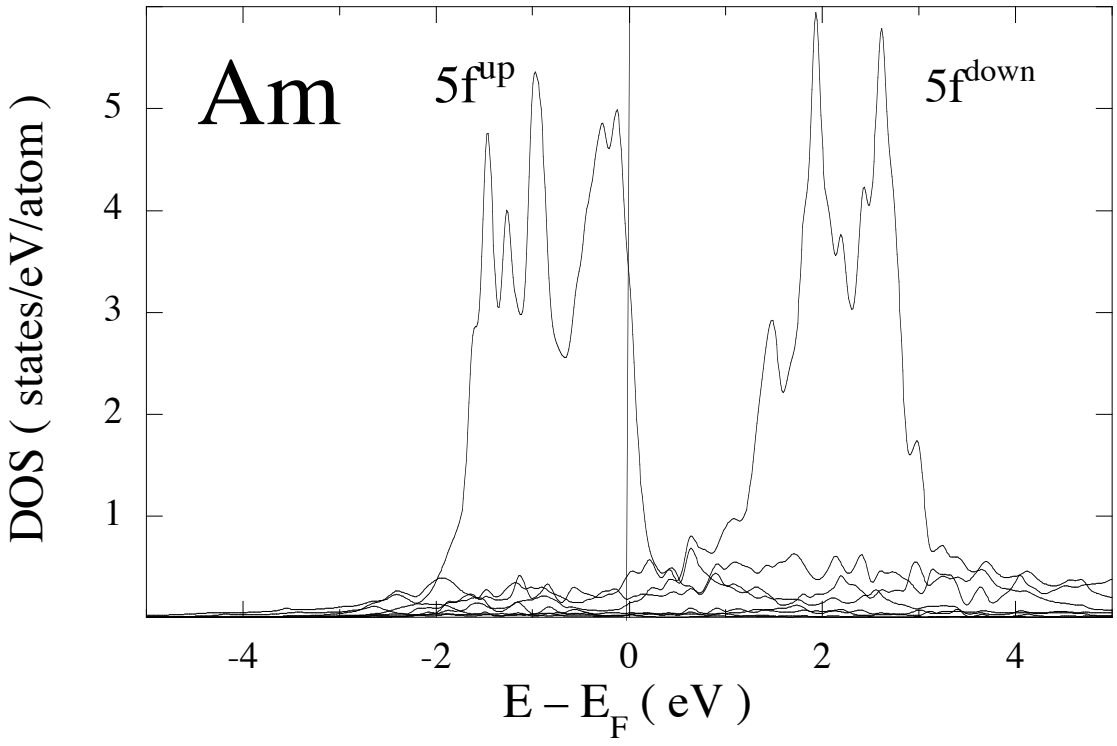
Am
5f^up
5f^down
DOS (states/eV/atom)
1
2
3
4
5
-4
-2
0
2
4
E – E_F (eV)

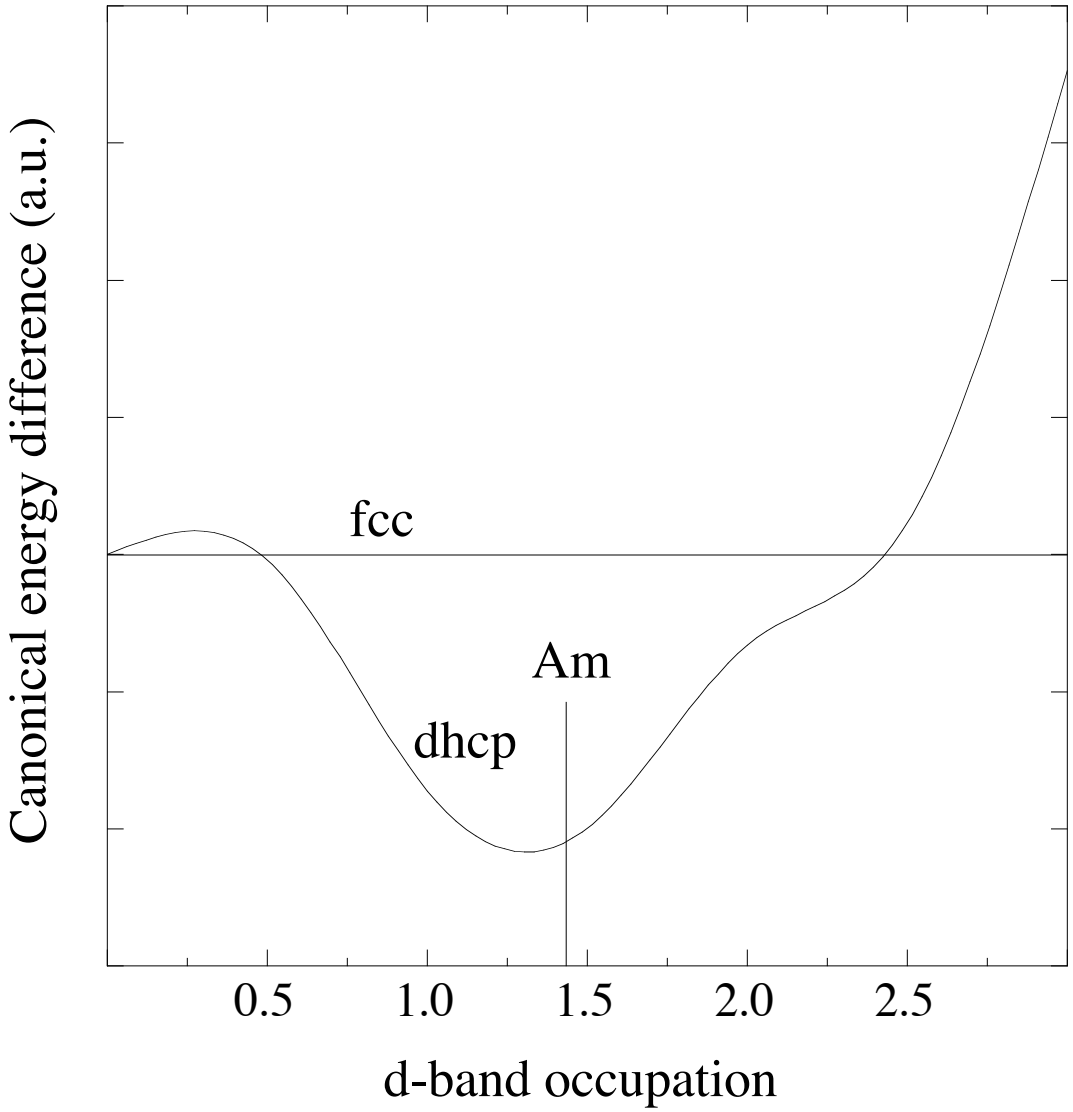
Canonical energy difference (a.u.)
fcc
Am
dhcp
0.5
1.0
1.5
2.0
2.5
d-band occupation

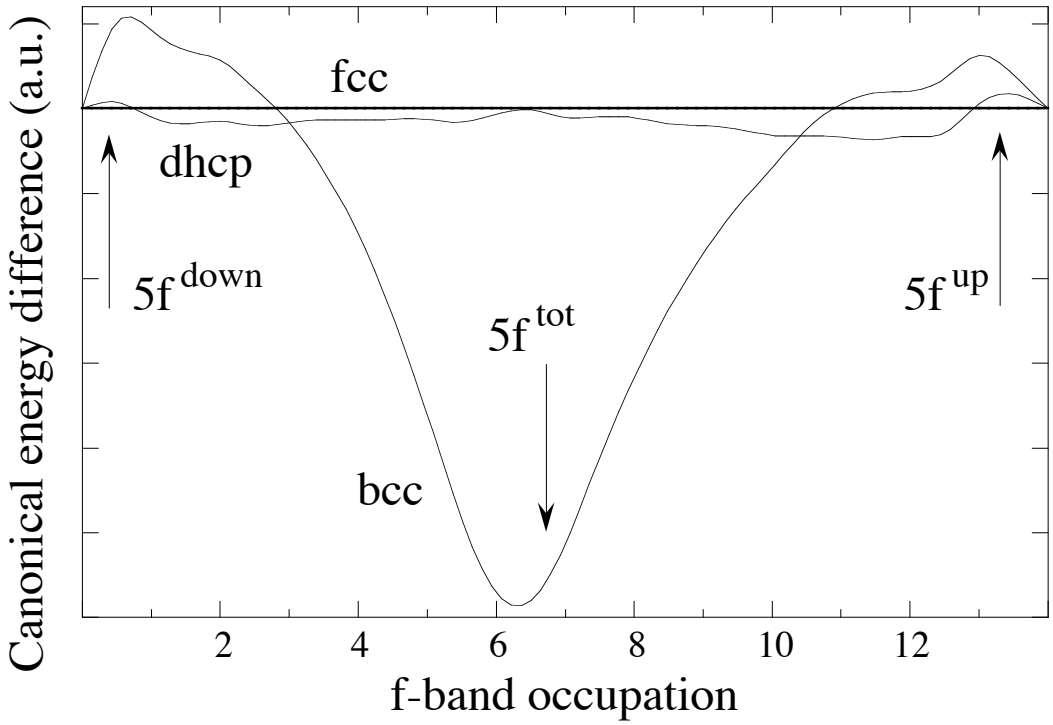
Canonical energy difference (a.u.)
fcc
dhcp
5f down
5f tot
5f up
bcc
2
4
6
8
10
12
f-band occupation